NANO LETTERS

2005
Vol. 5, No. 1
113−117

Bright and Stable Core–Shell Fluorescent Silica Nanoparticles

Hooisweng Ow,[†,||] Daniel R. Larson,[‡,||,⊥] Mamta Srivastava,[§] Barbara A. Baird,[§] Watt W. Webb,[‡] and Ulrich Wiesner[†,*]

Department of Materials Science and Engineering, School of Applied and Engineering Physics, Department of Chemistry and Chemical Biology, Cornell University, Ithaca, New York 14853

Received October 24, 2004

ABSTRACT

A class of highly fluorescent and photostable core–shell nanoparticles from a modified Stöber synthesis in the size range of 20–30 nm is described. These nanoparticles are monodisperse in solution, 20 times brighter, and more photostable than their constituent fluorophore, and are amenable to specific labeling of biological macromolecules for bioimaging experiments. The photophysical characteristics of the encapsulated fluorophores differ from their solution properties. This raises the possibility of tuning nanoparticle structure toward enhanced radiative properties, making them an attractive material platform for a diverse range of applications.

Fluorescent nanoparticles have tremendous promise as indicators and photon sources for a number of biotechnological and information technology applications such as biological imaging, sensor technology, microarrays, and optical computing.[1] These applications all require size-controlled, monodisperse, bright nanoparticles that can be specifically conjugated to biological macromolecules or arranged in higher-order structures. Nanoparticles with core−shell architecture have the added benefit of providing a robust platform for incorporating diverse functionalities into a single nanoparticle.[2]

We have developed a novel class of multifunctional silica-based fluorescent nanoparticles using a synthesis based on the Stöber method. The Stöber synthesis of colloidal silica, by which monodisperse nano- to micrometer sized silica particles may be obtained, was first described in 1968.[3] Van Blaaderen and co-workers first reported the covalent incorporation of organic fluorophores into Stöber colloidal silica and the synthesis of fluorescent silica nanoparticles in the hundreds of nanometers size range.[4] Comprehensive syntheses have since been performed to obtain plain or dye-doped Stöber colloidal silica ranging from tens to hundreds of nanometers in size.[5] Modifications using nonionic surfactants to improve monodispersity and sphericity in the lower size ranges have also been extensively studied.[6] Highly porous dye-labeled poly(organosiloxane) microgels with core−shell architecture have been reported, in which increased fluorescence intensity of the labeled fluorophore due to "caging effects" was observed.[7] To the best of our knowledge, however, none of the previous efforts have produced highly fluorescent silica nanoparticles in the 20−30 nm size range with brightness levels reaching those of semiconductor quantum dots and simultaneously enhanced photostability.[8] Here, we characterize highly fluorescent monodisperse silica nanoparticles, referred to as CU dots, with core−shell architecture consisting of a fluorophore-rich center protected within a siliceous shell that meet those requirements. For existing nanoparticle technology such as micelles, polyelectrolyte capsules, and liposomes, small-molecule loading into the core−shell construct is dependent upon diffusion rates.[9] The encapsulation process leading to the CU dots involves first covalent attachment of the dye molecules to a silica precursor to form the adduct of the core materials, followed by co-condensation with sol−gel precursor in specific order depending on the desired architecture. This approach affords versatility with regard to the placement of the dye molecules within the silica nanoparticle, for example as an intermediate layer or on the nanoparticle surface.

Fluorescence correlation spectroscopy (FCS) is used as a primary investigative tool to characterize these nanoparticles. FCS has now become a common tool for characterizing the properties of fluorescent moieties in solution.[10,11] This technique is particularly useful in the characterization of novel fluorescent nanoparticles because FCS can be used to measure the concentration, brightness, hydrodynamic radius, and monodispersity of the fluorescent probe in a single measurement, allowing for rapid characterization of probes in solution.[12]

* Corresponding author. E-mail: uli@ccmr.cornell.edu; Fax: (607)255-2365.
† Department of Materials Science and Engineering.
‡ School of Applied and Engineering Physics.
§ Department of Chemistry and Chemical Biology.
|| These authors contributed equally to this work.
⊥ Present address: Department of Anatomy and Structural Biology, Albert Einstein College of Medicine, Bronx, New York.

10.1021/nl0482478 CCC: $30.25
Published on Web 12/17/2004

We focus on the characterization of fluorescent silica nanoparticles with a radius of 15 nm. These nanoparticles are 20 times brighter than the constituent dye, are monodisperse in solution, and show improved photostability over the constituent dye. By examining the photophysical behavior of the intermediates of the synthesis process, we demonstrate that addition of the silica shell is critical in achieving the desired fluorescent properties of the particle. Furthermore, the hydrodynamic radius and the brightness of silica nanoparticles are comparable to water-soluble semiconductor nanocrystals (quantum dots), making silica nanoparticles an attractive alternative for applications requiring bright fluorescent probes. Finally, we present an application of CU dots for specific labeling of cell surface receptors.

The synthesis strategy of CU dots is based on a two-part process (see Figure 1A).[13] The organic dye molecules are first covalently conjugated to a silica precursor and condensed to form a dye-rich core. Silica sol−gel monomers are subsequently added to form a denser silica network around the fluorescent core material, providing shielding from solvent interactions which can be detrimental to photostability. This protocol is similar to what has been described by Ricka and co-workers as "heterogeneous nucleation", through which greater control over size monodispersity is obtained.[5a] In our approach, the seed for the heterogeneous nucleation consists of the dye-rich core. The versatility of this approach enables incorporation of various classes of fluorophores that cover the entire UV−vis absorption and emission spectrum (Figure 1C).

In the following we will concentrate on a particular CU dot with tetramethylrhodamine isothiocyanate (TRITC) as the encapsulated organic dye. The three distinct moieties in the synthesis process are the free dye (tetramethylrhodamine isothiocyanate, TRITC), the dye-rich core, and the complete core−shell particle. The hydrodynamic radius and the brightness of each species were determined from FCS measurements (Figure 2). The FCS curve for each moiety (TRITC, core, core/shell) was fitted to a single diffusion coefficient, indicating that the samples are monodisperse within the accuracy of the measurement (Figure 2A). TRITC has a diffusion coefficient of 0.21 μm^2/ms, in agreement with other reports,[14] corresponding to a hydrodynamic Stokes−Einstein radius of approximately 1.0 nm (Figure 2A, red circles). The core is only marginally larger than the free dye and has a radius of 2.2 nm (Figure 2A, green circles). After addition of the silica shell, the radius of the particle increases to 15 nm. Due to electron beam radiation degradation during TEM analysis, the dry silica nanoparticles may appear smaller than the hydrodynamic radius.[15] However, the size distribution characterized by FCS is corroborated by TEM data (Figure 1B), indicating that the nanoparticles are well-approximated as hard spheres in solution. The smallest well-defined core−shell particles we obtained so far had a hydrodynamic radius of 12 nm.

The amplitude of the autocorrelation provides the number of the diffusing species, and the average count rate is a measure of the photons collected from the optically defined focal volume. One can therefore obtain the count rate per molecule for each diffusing species, which is a direct measure of the brightness of a probe. The brightness of the three synthesis stages at the same excitation power is shown in Figure 2B. The brightness of the core is actually less than that of free TRITC, suggesting that the dense dye-rich core is heavily quenched compared to the free dye. However, upon addition of an outer, dye-free silica shell to the core, the brightness increases by a factor of 30. This enhancement is likely due to a change in the radiative properties of the dye and is the subject of continued investigation.

One possible contribution to the enhancement of brightness upon addition of the silica shell is protection of the fluorophore from the solvent. The solvent accessibility of the core/shell particles is shown in Figures 3 A−C as a shift in the excitation and emission spectrum upon solvent exchange. The excitation and emission spectra of free dye

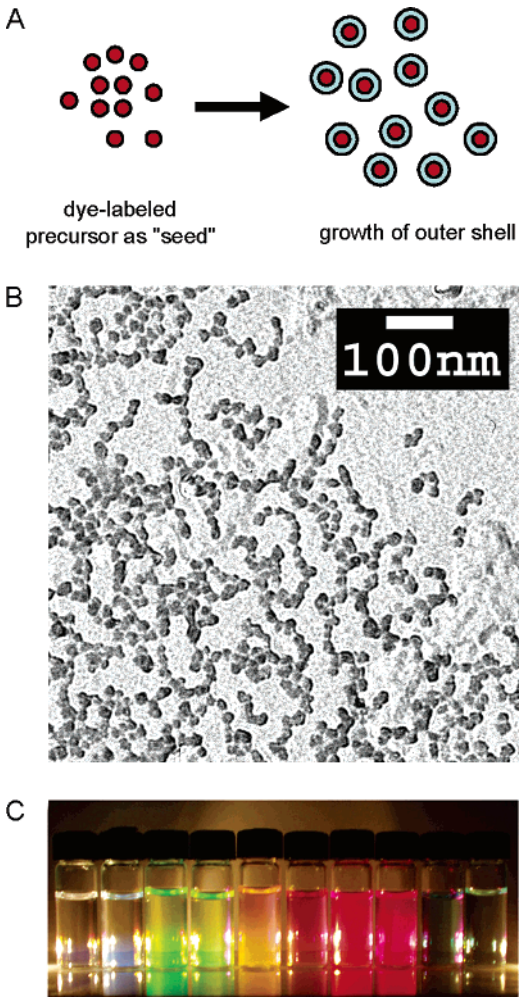

Figure 1. Fluorescent core−shell silica nanoparticles. (A) Schematic representation of the synthesis of core−shell fluorescent silica nanoparticles. (B) The resultant 30 nm particles as characterized by transmission electron microscopy (TEM). Because of the slow water evaporation process used to prepare the TEM grids, the particles are aggregated in this image. (C) The synthesis protocol can be extended to incorporate organic dyes with different spectral characteristics, covering the entire UV−vis absorption and emission wavelengths. Organic dyes incorporated from left to right are Alexa 350, *N*-(7-(dimethylamino)-4-methylcoumarin-3-yl), Alexa 488, fluorescein isothiocyanate, tetramethylrhodamine isothiocyanate, Alexa 555, Alexa 568, Texas Red, Alexa 680, and Alexa 750.

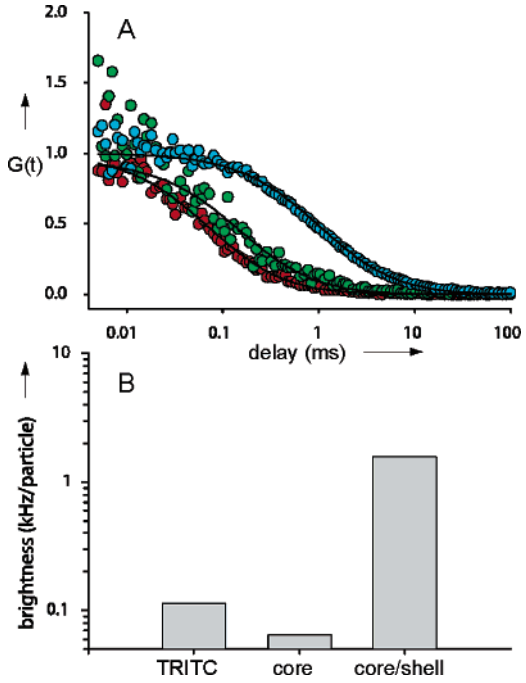

Figure 2. Comparison of nanoparticle synthesis intermediates. (a) FCS curves for TRITC (red circles), the core (green circles), and the core−shell (blue circles). The curves are normalized for display, and each curve is fit with a single diffusion coefficient. The diffusion coefficients are 0.21 μm^2/ms, 0.098 μm^2/ms, and 0.014 μm^2/ms for TRITC, core, and core/shell, respectively. (b) The relative brightness, measured as count rate/particle, is also determined from the FCS curves. Excitation: 900 nm. Power: 1.4 mW.

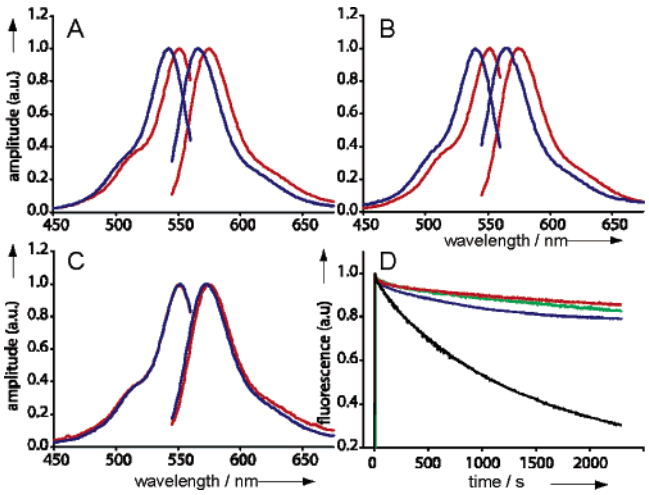

Figure 3. Solvent accessibility and photobleaching behavior of nanoparticle synthesis intermediates. Panels A−C: Excitation and emission spectra of nanoparticle intermediates ((A) TRITC; (B) core; (C) core/shell) in ethanol (blue) and water (red). (D) Photobleaching behavior of nanoparticle intermediates (blue, TRITC; green, core; red, core/shell) and fluorescein (black). All curves in panels A−D are normalized by the peak values.

and core exhibit a red shift after exchange from ethanol to water (Figures 3A, B). However, the silica nanoparticle spectra show little, if any, spectral shift (Figure 3C), suggesting that the nanoparticle shell is largely impermeable to solvent.

In addition, photobleaching is known to be dependent on solvent interactions and is thought to occur as a bimolecular

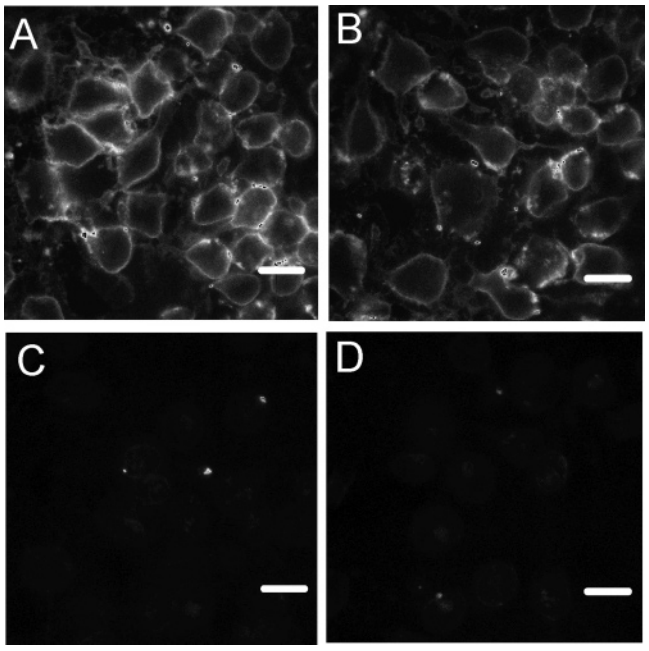

Figure 4. Labeling of mucosal mast cell receptors with silica nanoparticles. Panels A and B are micrographs of rat basophilic leukemia (RBL) mast cells specifically labeled with fluorescent silica nanoparticles functionalized with immunoglobulin E (IgE). Panels C and D are micrographs from negative control experiments where the IgE receptor is blocked with unlabeled IgE. Scale bar: 10 μm.

reaction between the dye and, for example, dissolved oxygen.[16,17] Figure 3D shows the photobleaching behavior of the dye, core, core−shell, and fluorescein, another organic dye often used in photobleaching studies. Both the core and the core−shell bleach less than free TRITC, and the core−shell shows reduced photobleaching compared to the core. It is interesting to note that TRITC is a fairly photostable fluorophore, hence the difference in photostability between free dyes and silica nanoparticles is small. For comparison, Figure 3D also shows the bleaching behavior of fluorescein isothiocyanate, a fast-bleaching fluorophore.[16] Taken together with the solvent exchange results, these measurements indicate that the dye in the CU dots is relatively inaccessible to solvent, and that this protection affords increased photostability. Photostability is a particularly important criterion when using nanoparticles as fluorescent markers in complex biological environments, where it is often desirable to observe markers for extended periods of time against the background of intrinsic cellular emissions.

We demonstrate the potential of these silica nanoparticles as markers for biological imaging by labeling the FcϵRI receptor of rat basophilic leukemia (RBL) mast cells. Antibody immunoglobulin E (IgE) and its cell surface receptor, FcϵRI, are known to form a reversible but tight complex.[18] IgE was adsorbed onto the surface of the CU dots at the optimum ratio of 1:1, established via iterations of binding assays. Figure 4A, B shows typical labeling of RBL cells with antibody-adsorbed silica nanoparticles. In equatorial sections of the cells, only the periphery of the cell was labeled, as expected for the transmembrane FcϵRI receptor. As a negative control, RBL mast cells were

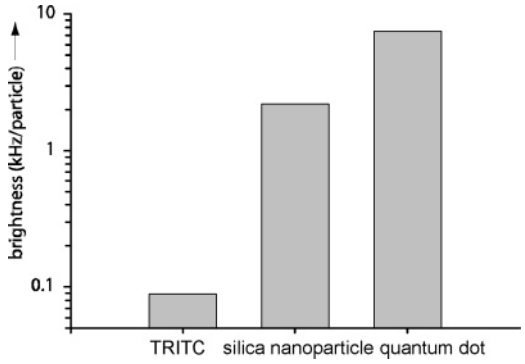

Figure 5. Brightness comparison for TRITC, silica nanoparticles and quantum dots. The brightness values are obtained from FCS measurements of the count rate/particle at intensities below which fluorescence saturation and photobleaching occur. Excitation: 860 nm. Power: 0.4 mW.

presensitized overnight with IgE before incubation with bare silica nanoparticles. In this case, very little peripheral staining was observed, indicating minimal nonspecific interaction between the silica nanoparticles and the cell surface (Figure 4C, D). Labeling specificity is critical for most biological applications, but specific binding is especially crucial for applications such as single-particle tracking where motions of cell surface components are monitored over extended periods of time. At present, we are able to achieve sufficient specificity via physical adsorption of IgE to the nanoparticle. However, one would expect greater control through covalent conjugation of biomolecules, which can be accomplished by applying surface chemical functionality such as carboxyls or amines on the silica nanoparticles using well-established silane coupling chemistry.

Finally, we made a direct comparison between TRITC, CU dots, and water-soluble quantum dots. The radiative processes of quantum dots and silica nanoparticles are likely to be quite different: quantum dot excitation and emission occur primarily through a single exciton, while silica nanoparticles may have multiple dye molecules absorbing and emitting independently. Nonetheless, the size and brightness of each probe can be directly compared, and these properties are often the most critical for many applications. The hydrodynamic radius of 15 nm for silica CU dots (Figure 2A) is practically identical to that of water-soluble CdSe/ZnS quantum dots ($r = 14$ nm).[12] Figure 5 compares the brightness of free dye, silica nanoparticles, and quantum dots with a peak fluorescence at 577 nm (counts/particle for silica nanoparticles and quantum dots and counts/molecule for TRITC). Both quantum dots and CU dots are one to two orders of magnitude brighter than free TRITC. On the other hand, the difference between the silica nanoparticles and quantum dots is only a factor of two to three and may be overcome with improved synthetic methods for the silica nanoparticles.

We have described a novel class of 30 nm fluorescent silica nanoparticles, CU dots, which are bright, monodisperse in solution, photostable, and amenable to specific labeling of biological macromolecules. In addition, the well-developed conjugation chemistry and biological compatibility of silica make silica nanoparticles a viable technology for a wide range of imaging applications in living biological systems.

Moreover, fluorophores within the silica nanoparticle exhibit photophysical properties that are different from their solution properties, for example increased photostability. The altering of photophysical properties of the constituent dye molecules raises the possibility of specifically tuning the physical structure of the nanoparticle to attain novel or enhanced radiative properties of the fluorophore. Likewise, understanding the local structure and interactions within the silica nanoparticles also enables the development of nanoparticles with controlled material properties. Work along these lines is now in progress in our laboratory.

Acknowledgment. This publication was developed under the auspices of the Cornell University Center for Biotechnology, a New York State Center for Advanced Technology supported by New York State and industrial partners. This work was also supported by NSF grant DBI-0080792, NIBIB/NCRR-NIH grant 9 P41 EB001976-16 (D.R.L., W.W.W), and in part by the Nanobiotechnology Center (NBTC), an STC Program of the National Science Foundation under Agreement No. ECS-9876771. We gratefully acknowledge the support of Philip Morris USA. We also thank Marcel Bruchez at Quantum Dot Corporation for providing the quantum dots.

Supporting Information Available: Experimental techniques and materials. This material is available free of charge via the Internet at http://pubs.acs.org.

References

(1) (a) Jaiswal, J. K.; Mattoussi, H.; Mauro, J. M.; Simon, S. M. *Nature Biotechnol.* **2003**, *21*, 47. (b) Lingerfelt, B. M.; Mattoussi, H.; Goldman, E. R.; Mauro, J. M.; Anderson, G. P. *Anal. Chem.* **2003**, *75*, 4043. (c) Goldman, E. R.; Clapp, A. R.; Anderson, G. P.; Uyeda, H. T.; Mauso, J. M.; Medintz, I. L.; Mattoussi, H. *Anal. Chem.* **2004**, *76*, 684.

(2) (a) Jackson, J. B.; Halas, N. J. *J. Phys. Chem. B* **2001**, *105*, 2743. (b) Lal, S.; Taylor, R. N.; Jackson, J. B.; Westcott, S. L.; Nordlander, P.; Halas, N. J. *J. Phys. Chem. B.* **2002**, *106*, 5609. (c) Jackson, J. B.; Westcott, S. L.; Hirsch, L. R.; West, J. L.; Halas, N. J. *Appl. Phys. Lett.* **2003**, *82*, 257.

(3) Stöber, W.; Fink, A. *J. Colloid Interface Sci.* **1968**, *26*, 62.

(4) van Blaaderen, A.; Vrij, A. *Langmuir* **1992**, *8*, 2921.

(5) (a) Nyffenegger, R.; Quellet, C.; Ricka, J. *J. Colloid Interface Sci.* **1993**, *159*, 150. (b) Verhaegh, N. A. M.; van Blaaderen, A. *Langmuir* **1994**, *10*, 1427.

(6) (a) He, X.; Wang, K.; Tan, W.; Li, J.; Yang, X.; Huang, S.; Li, D.; Xiao, D. *J. Nanosci. Nanotechnol.* **2002**, *2*, 317. (b) Santra, S.; Zheng, P.; Wang, K.; Tapec, R.; Tan, W. *Anal. Chem.* **2001**, *73*, 4988. (c) Zhao, X.; Bagwe, R. P.; Tan, W. *Adv. Mater.* **2004**, *16*, 173.

(7) Graf, C.; Schärtl, W.; Fischer, K.; Hugenberg, N.; Schmidt, M. *Langmuir* **1999**, *15*, 6170.

(8) (a) Murray, C. B.; Norris, D. J.; Bawendi, M. G. *J. Am. Chem. Soc.* **1993**, *115*, 8706. (b) Michalet, X.; Pinaud, F.; Lacoste, T. D.; Dahan, M.; Bruchez, M. P.; Alivisatos, A. P.; Weiss, S. *Single Mol.* **2001**, *4*, 261.

(9) Jungmann, N.; Schmidt, M.; Ebenhoch, J.; Weis, J.; Maskos, M. *Angew. Chem., Int. Ed.* **2003**, *42*, 1714.

(10) Magde, D.; Elson, E.; Webb, W. W. *Phys. Rev. Lett.* **1972**, *29*, 705.

(11) (a) Hess, S. T.; Huang, S.; Heikal, A. A.; Webb, W. W. *Biochem.* **2002**, *41*, 697. (b) Thompson, N. L. *Topics in Fluorescence Spectroscopy: Techniques*; Plenum Press: New York, 1991; pp 337−378.

(12) (a) Larson, D. R.; Zipfel, W. R.; Williams, R. M.; Clark, S. W.; Bruchez, M. P.; Wise, F. W.; Webb, W. W. *Science* **2003**, *300*, 1434.

(b) Minard-Basquin, C.; Weil, T.; Hohner, A.; Rädler, J. O.; Müllen, K. *J. Am. Chem. Soc*. **2003**, *125*, 5382. (c) Erhardt, R.; Zhang, M.; Böker, A.; Zettl, H.; Abetz, C.; Frederik, P.; Krausch, G.; Abetz, V.; Müller, A. H. E. *J. Am. Chem. Soc*. **2003**, *125*, 3260.
(13) Ow, H.; Wiesner, U., U.S. Patent Application file#: 1153.081US1, 2002; for a detailed description of the synthesis, the interested reader is referred to a forthcoming publication of the same authors.
(14) Schwille, P.; Haupts, U.; Maiti, S.; Webb, W. W. *Biophys J.* **1999**, *77*, 2251.
(15) van Helden, A. K.; Jansen, J. W.; Vrij, A. *J. Colloid Interface Sci*. **1981**, *81*, 354.
(16) Song, L.; Hennink, E. J.; Young, I. T.; Tanke, H. J. *Biophys. J*. **1995**, *68*, 2588.
(17) Soper, S. A.; Nutter, H. L.; Keller, R. A.; Davis, L. M.; Shera, E. B. *Photochem. Photobiol*. **1993**, *57*, 972.
(18) Kulczycki, A., Jr.; Metzger, H. *J. Exp. Med.* **1974**, *140*, 1676.

NL0482478